On physical mechanisms in two– and three–dimensional separations

F. T. Smith

Phil. Trans. R. Soc. Lond. A 2000 **358**, 3091-3111
doi: 10.1098/rsta.2000.0698

10.1098/rsta.2000.0698

THE ROYAL SOCIETY

On physical mechanisms in two- and three-dimensional separations

By F. T. Smith

Department of Mathematics, University College London, Gower Street, London WC1E 6BT, UK

Some of the physical mechanisms that arise in interactions, upstream influence and separation are discussed for boundary layers and internal motions. Mechanism 1 involves pressure–displacement interaction, stemming from the Goldstein singularity and the issue of its removal. At least six other mechanisms, 2–7, arise in more recent studies for two- and three-dimensional flows. These are in blade–wake rotary flows, where streamwise periodicity, inner–outer interactions at very low incidence, and leading-edge jump effects enter the reckoning, and in surface-mounted roughness flows, concerning three-dimensional upstream influence, pressure feedback and longitudinal (e.g. horseshoe) vortex formation.

Keywords: separations; roughness; rotary blades; horseshoe vortices; boundary layers; fluid dynamics

1. Introduction

The invited talk that formed the basis for this article was entitled 'Repercussions from Goldstein's (1948) paper', a tribute to Sydney Goldstein's magnificent contribution 50 years previously. This article is also intended as a tribute by the present author to the great Sir James Lighthill, a colleague who died eight days after the end of the discussion meeting.

The emphasis here in considering the repercussions from Sydney Goldstein's paper is on physical mechanisms in fluid flows at high Reynolds numbers. The present paper is in three main parts. The first part, in § 2, gives the line of theoretical reasoning developed from 1948 onwards. It may be sparse and biased but it leads to physical mechanism 1 of interaction and upstream influence. It also provides the basis for the second and third parts, which concern more current work. The second part is described in § 3, on recent work concerning rotary multi-blade flows, while the third part, in § 4, is on three-dimensional surface-mounted roughness flows, as studied theoretically and computationally over the last 20 years or so as well as much more recently. These second and third parts point to at least six more distinct physical mechanisms, 2–7, some of which are familiar and some less so. The list of mechanisms found is far from comprehensive. They are mostly built up from studies of small-scale separations in two and three dimensions, but they also include breakaway three-dimensional separation of a vortex sheet from a body surface, for example. Again, mechanisms 5 and 7 are specifically three-dimensional. Brief final comments are added in § 5.

PHILOSOPHICAL TRANSACTIONS OF THE ROYAL SOCIETY A MATHEMATICAL, PHYSICAL & ENGINEERING SCIENCES

The many applications of high-Reynolds-number theory and computation can largely be taken as read. In the particular context of rotary multi-blade flows (§ 3), however, they include aerodynamic configurations (for example helicopters, other rotorcraft, propellers) and internal flows (in engines, turbine blades) in some settings, domestic appliances (food mixers and blenders, some types of bean grinders), garden appliances (such as hover mowers), nature (as in airborne seed travel, e.g. sycamore seeds), fans (in cars, ovens or buildings), industrial mixers (e.g. concrete mixers and larger containers), and so on. This is quite apart from the many applications to rotary motions in geophysical and related fluid dynamics. Similarly, the context of surface-roughness flows (§ 4) has numerous practical applications, for instance to blade and airfoil surface manufacture and to design of local lift or mixing devices, such as the vortex generator and the Gurney flap. We work in terms of non-dimensional scaled quantities based on a characteristic length-scale and velocity scale, for instance the distance from a leading edge and the freestream velocity, respectively. This will become clearer in context, although the particular scalings involved are omitted in order to highlight the mechanisms themselves. Generally, the non-dimensional velocity components are u, v, w, in corresponding Cartesian coordinates x, y, z (or scaled X, Y, Z or polars r, Y, θ), which are streamwise, normal and spanwise in conventional notation, the pressure is p, time is t and Re is the large global Reynolds number. The work is mostly for an incompressible fluid and laminar motion.

2. Direct repercussions from Goldstein's singularity: mechanism 1

The 1948 paper was on the classical laminar-boundary-layer flow near a position of 'separation', envisaged as the point at which the scaled skin friction tends to zero, under an adverse pressure gradient. Goldstein was motivated by 'a careful numerical computation by Hartree for a linearly decreasing velocity distribution outside the boundary layer' (see also Hartree 1937), and mentioned also an earlier computation by Howarth (1938). 'Hartree was convinced that there was a singularity in the solution at the position of separation', and Goldstein 'undertook to try to find some formulae that would hold near this singularity and would help in finishing the computation'. Goldstein sets the scene for us, referring to flow at a large Reynolds number along an immersed solid surface, where a boundary layer is formed through which the velocity (u) rises rapidly from zero at the surface to its value (U) in the main stream. The approximate equations for the two-dimensional flow of a fluid in a boundary layer are

$$u = \frac{\partial \psi}{\partial y}, \tag{2.1 a}$$

$$v = -\frac{\partial \psi}{\partial x}, \tag{2.1 b}$$

$$u\frac{\partial u}{\partial x} + v\frac{\partial u}{\partial y} = -p'(x) + \frac{\partial^2 u}{\partial y^2} \tag{2.1 c}$$

(his eqn (1) with ρ, ν now replaced by unity). From the mainstream, $-p'(x) = UU'(x)$, since the boundary conditions here require $u \to U(x)$ as $y \to \infty$, as well as $u = v = 0$ at $y = 0$ and u being given as a function of y at some initial value of x. Parabolicity in x is assumed in this (quasi-) attached-flow strategy, ahead of the singularity position. Near this position, where $x \to 0-$ say, Goldstein introduced the now familiar transformed coordinates $|x|^{1/4}$, $y/|x|^{1/4}$ near the wall, reflecting the $O(|x|^{1/4})$ sublayer thickness and, implicit in the subsequent boundary conditions on similarity functions, the presence of two zones in the normal direction for the local description of the boundary layer. He then went on, with the stress on nonlinearity, to find the similarity functions involved in the details of the singularity (see also Stewartson 1958), which predicts a square-root irregularity in the scaled skin friction τ and boundary-layer displacement δ.

A neat demonstration that the singularity is possible was given later by Curle (1962). Differentiation of (2.1 *c*) twice with respect of y gives, along $y = 0$, $\partial_x(\tau^2) = 2u_{yyyy}$, where τ is $\partial u/\partial y$ evaluated at zero y. Hence, if the right-hand side is non-zero at $x = 0-$, which is the general case, then

$$\tau \propto |x|^{1/2}, \tag{2.2}$$

which retrieves Goldstein's fundamental finding for the scaled skin friction. This demonstration is one item in an excellent review on laminar separation by Brown & Stewartson (1969), who include two more main items as far as this article is concerned as well as several others of alternative interest, for example on compressible boundary layers. Brown & Stewartson (1969) note the result that the local variation in δ is $-\tau(x)/p'(x)$, yielding a square-root behaviour in δ from (2.2) when p' is specified as above. But, instead, regularity can be ensured by requiring $\delta(x)$ to be regular and treating $p'(x)$ as unknown. To quote from Brown & Stewartson (1969):

> In fact, the first numerical integration through the point of separation was carried out, by Catherall & Mangler (1966), using this result. Their integrations were started at stagnation with a prescribed pressure gradient, but at an appropriate point near separation they stopped specifying the pressure gradient *a priori* and instead smoothly joined the displacement thickness to a parabolic or cubic form. From this point on the pressure gradient was regarded as one of the unknowns and determined step-by-step numerically. They found that the solution passed smoothly through separation and a region of reversed flow was set up downstream: it was even possible to achieve reattachment.

That is from the boundary layer alone. Concerning interaction, Brown & Stewartson (1969) observed that the pressure gradient in the mainstream depends on δ through the relation $p'(x) = (M_\infty^2 - 1)^{-1/2}\delta''(x)$, from linearized theory (Ackeret) if the mainstream is supersonic with local Mach number $M_\infty > 1$. A similar relation holds locally in subsonic flow. A start on a theory incorporating interaction with the flow just outside the boundary layer was made earlier by Lighthill (1953) (after Oswatitsch & Wieghardt's (1941) outline), who obtained the initial pressure rise or fall associated with such interactive upstream influence in the form

$$p \propto \exp(Kx), \tag{2.3}$$

where $K \propto |M_\infty^2 - 1|^{3/8} Re^{3/8}$ is the Lighthill eigenvalue. This provides *mechanism 1*; it is equivalent to the triple-deck mechanism of upstream influence and/or interaction, and it also arises similarly in subsonic motions, involving the same 3/8 streamwise length scaling.

The next major step can be counted as Stewartson's (1970), asking if the singularity (2.2) at separation is removable or not. He remarks that 'many numerical integrations support Goldstein's theory of the structure of the solution of a laminar boundary layer near the point of separation 0 when the mainstream is prescribed, and in particular confirm that the solution is singular there.' Stewartson (1970) examines the local effects with interaction present, building on Goldstein's two normal zones mentioned earlier and finding the normalized governing equation,

$$B^2 + X = \int_X^\infty \frac{B''(s)\,\mathrm{d}s}{(s-X)^{1/2}}, \tag{2.4}$$

for the scaled skin friction $B(X)$, which is proportional to the negative displacement variation. The left-hand side in (2.4) points to the Goldstein square-root form (2.2) at large negative X, whereas the right-hand side is the interactive contribution for subsonic motion, a similar contribution holding in the supersonic range, intended to remove, if possible, the incoming square-root behaviour. Stewartson (1970) indicates, however, that there is no physically sensible solution of (2.4) or its supersonic companion, this pointing to the conclusion that the Goldstein singularity is not removable. The 1970 paper also observes, on the other hand, the equally important point that the balance between the B^2 term and the integral in the supersonic analogue of (2.4) yields upstream influence, contrary to the classical attached-flow assumption; this balance leads again to mechanism 1.

The Goldstein singularity arising in the above attached-flow strategy leaves us with the following choices or possibilities.

(a) **The strategy does not work.** In this case we must start again, leading on to the study of upstream influence, pressure–displacement interaction, triple-deck theory, interactive boundary layers and related ideas (see Lighthill (1953), Neiland (1969), Messiter (1970), Stewartson & Williams (1969), and many subsequent investigations). Recent work is described in §§ 3 and 4.

(b) **The strategy does work.** The major case so far is for condensed flow over a surface roughness (Smith & Daniels (1981); see also below). Again, recent work is in the next two sections of the paper.

(c) **The strategy might work.** This is for weakly singular cases, leading to marginal separation (see Ruban (1981, 1982), Stewartson *et al.* (1982), Smith (1982), and subsequent studies). A recent development is contained in § 4.

Concerning possibility (b), Smith & Daniels (1981) showed that a removal of Goldstein's singularity at separation occurs in external or internal flow over an isolated roughness within a near-wall sublayer. The problem of interest there is to solve (2.1) but with the boundary condition

$$u \sim y + hF(x) \quad \text{as } y \to \infty, \tag{2.5}$$

for the effects of the roughness on the otherwise uniform shear flow in the sublayer. No slip is required at zero y. The given roughness height $hF(x)$ plays the role of a given negative displacement, while the pressure $p(x)$ is an unknown function of x (cf. Catherall & Mangler 1966). The parameter h can be varied from zero to infinity. There is no significant upstream influence in the system (2.1) with (2.5) as

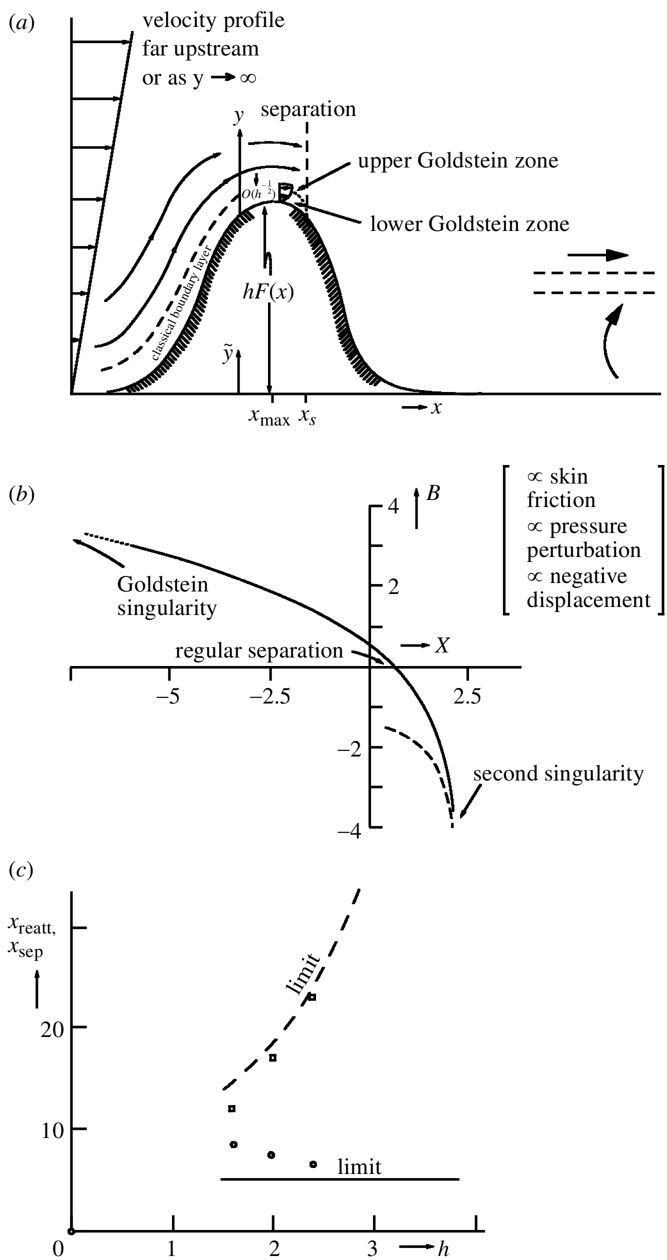

Figure 1. (a) Structure of the wall layer flow past a planar roughness when the height parameter h is large, including separation. (b) Removal of the Goldstein singularity by the solution $B(X)$ of (2.6). (c) Comparisons, for increasing h, between computations (squares, circles) and large-h theory (limit) for the separation and reattachment positions.

long as the flow is forward in x, the new physics required for significant upstream influence for sublayer flows being addressed in § 4. Moreover, separation or flow reversal, if encountered, is regular, because of the unknown-pressure setting. On the other hand, suppose h is large. Then, at heart, (2.5) becomes $u \to hF(x)$, giving, in (2.1), a classical formation with $p(x) = -h^2F^2(x)/2$ (Bernoulli) specified in the attached flow on the windward face of the roughness and just beyond (see figure 1*a*). On the leeward face, however, the deceleration due to decreasing $F(x)$ generally drives this classical thin-layer solution into the Goldstein singularity (2.2) under finite adverse pressure gradient. Given the above setting, the singularity must, therefore, be removable. The flow structure in the local removal, following the Goldstein double-zone, is rather complex, as shown in fig. 2 of Smith & Daniels (1981), but it hinges first on the interactive equation

$$\frac{\mathrm{d}}{\mathrm{d}X}(B^2 + X) = -\int_{-\infty}^{X} \frac{B''(s)\,\mathrm{d}s}{(X-s)^{1/2}}, \tag{2.6}$$

in normalized form, derived from (2.1), (2.5). The minus sign on the right-hand side of (2.6) arises from the local pressure–displacement law $P = +B$, consistent with the Bernoulli relation. This sign is crucial, and different from those typical in broader-scale motions, such as in the supersonic companion of (2.4), for example, in that (2.6) rules out upstream influence and yields a unique physically sensible solution (figure 1*b*). It terminates in another singularity but that also is removable, leading on next to complete breakaway of the thin layer from the roughness surface. The breakaway is controlled essentially by (2.1) subject to the new pressure–displacement relation

$$p = A + x, \tag{2.7 a}$$

where now

$$u \sim y + A \quad \text{as } y \to \infty, \tag{2.7 b}$$

locally. This has the finite adverse pressure gradient of unity entering upstream, where A is negligible in (2.7 *a*), whereas far downstream the effective displacement, $-A$, increases like x, under negligible p in (2.7 *a*), as in Smith & Daniels's (1981) figs 5 and 6. Comparisons with results at finite h values are presented in figure 1*c*.

Concerning possibility (c), marginal separation occurs if the Goldstein singularity appears only weakly, with a small constant of proportionality in (2.2). In flow near a rounded leading edge there is a critical angle of incidence, below which τ has a positive minimum and above which τ tends to zero as in (2.2) (see fig. 1 in Stewartson *et al.* (1982)). For angles sufficiently close to that critical value, the fundamental equation of marginal separation is, for subsonic flows,

$$B^2 - X^2 + \Gamma = \int_{X}^{\infty} \frac{B''(s)\,\mathrm{d}s}{(s-X)^{1/2}}, \tag{2.8}$$

where the constant Γ represents deviations from the critical value. For large negative Γ values, B is approximately $(X^2 + |\Gamma|)^{1/2}$, confirming a positive minimum, while for large positive Γ a square-root singularity reappears. The sign on the right-hand side is as in (2.4), but, crucially, the forcing term on the left-hand side is different, because of the marginal state. This allows physically sensible solutions to persist up to a finite value of Γ, some even admitting a small local separation eddy, as well as non-uniqueness. There are many interesting subsequent works in the area, including two and three dimensionality and unsteadiness (see, for example, Brown 1985; Elliott & Smith 1985; Timoshin 1997; Zametaev & Kravtsova 1998; Kluwick 1998).

PHILOSOPHICAL TRANSACTIONS OF THE ROYAL SOCIETY A MATHEMATICAL, PHYSICAL & ENGINEERING SCIENCES

3. Multi-blade flows: mechanisms 2–4

This recent and continuing research is motivated by the question of what happens to laminar boundary layers on rotary blades. We address four aspects below.

(*a*) *Rotary blades (and mechanisms 2 and 3)*

The first aspect is in the contribution by Smith & Timoshin (1996*a*). They describe the wide variety of practical applications, which include all those listed in the final paragraph of § 1, although paramount among those in technological terms is probably the helicopter-blade application. The above paper considers typically a rotating configuration of thin blades, of characteristic thickness comparable with that of the rotary three-dimensional boundary layers, with or without an incident uniform stream. Inside these layers, the three-dimensional boundary-layer equations hold, with α unity,

$$\frac{\partial u}{\partial r} + \frac{\alpha u}{r} + \frac{\partial V}{\partial Y} + \frac{1}{r}\frac{\partial w}{\partial \theta} = 0, \tag{3.1 a}$$

$$\frac{\partial u}{\partial t} + \frac{u\partial u}{\partial r} + V\frac{\partial u}{\partial Y} + \frac{w}{r}\frac{\partial u}{\partial \theta} + \alpha\left(2w - \frac{w^2}{r}\right) = -\frac{\partial P}{\partial r} + \frac{\partial^2 u}{\partial Y^2}, \tag{3.1 b}$$

$$\frac{\partial w}{\partial t} + \frac{u\partial w}{\partial r} + V\frac{\partial w}{\partial Y} + \frac{w}{r}\frac{\partial w}{\partial \theta} + \alpha\left(-2u + \frac{wu}{r}\right) = -\frac{1}{r}\frac{\partial P}{\partial \theta} + \frac{\partial^2 w}{\partial Y^2}, \tag{3.1 c}$$

in scaled terms and in a rotating frame, subject to

$$\text{zero slip on the blades,} \tag{3.1 d}$$

$$\text{regularity in the wakes,} \tag{3.1 e}$$

$$\text{far-field } (u, w) \to (0, r) + (\cos(\theta - t), -\sin(\theta - t))G, \tag{3.1 f}$$

$$\text{periodicity in } \theta. \tag{3.1 g}$$

In (3.1 *b*) and (3.1 *c*), P is prescribed, as $-r^2/2$, to within a constant, while in (3.1 *f*) the constant G is proportional to the incident speed, which provokes an unsteady response in general.

Condition (3.1 *g*) provides *mechanism 2*, as it makes each blade and wake flow interact with all the others.

Furthermore, *mechanism 3* arises if the configuration is non-symmetric in Y for instance. It stems from the motion outside the thin rotary layers above and so involves Laplace's equation for the small induced pressure $\tilde{p}$ in three dimensions (r, θ, y) subject to

$$\left.\frac{\partial \tilde{p}}{\partial y}\right|_{y=0\pm} = -\left[\frac{\partial}{\partial t} + G\cos(\theta - t)\frac{\partial}{\partial r} + \left(1 - \frac{G\sin(\theta - t)}{r}\right)\frac{\partial}{\partial \theta}\right]V|_{Y\to\pm\infty}, \tag{3.2}$$

following on from the far-field constraint (3.1 *f*). With non-symmetry present, the inner viscous and the outer inviscid problems of (3.1), (3.2) must interact in order for condition (3.1 *e*) to be satisfied in each gap. More on this is given in the following subsection.

Three-dimensional flow solutions, marched outwards from a central hub, are presented in the above paper mostly for radial blades, under the assumptions of hovering motion (zero G, admitting a steady flow description) and symmetry in Y, y

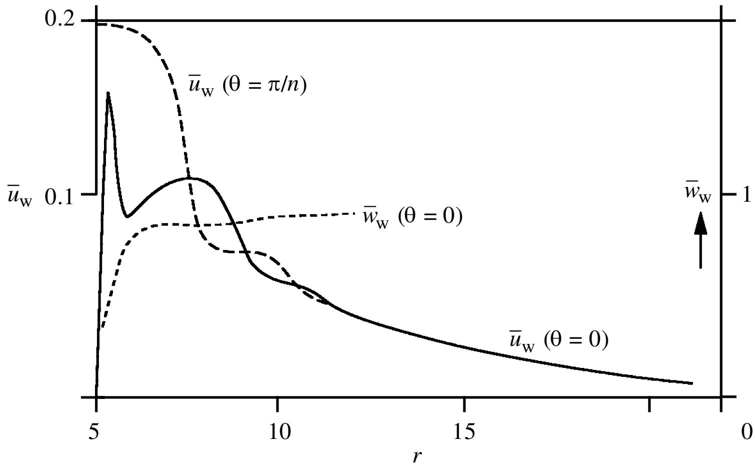

Figure 2. Outboard-marching results for (3.1 a)–(3.1 g) with zero G, Y-symmetry and n bounded blades of radius 5. Three-dimensional blade-tip effects are seen in the induced centreline velocities $\bar{u}_w$, $\bar{w}_w$ versus radius r at the θ values indicated. Here $n = 2$.

(there is then no inner–outer interaction). Numerous special or limiting cases are also examined, for instance short blades or long gaps. The solutions are given both for radially unbounded blades and for radially bounded ones (see figure 2), the latter exhibiting spatial oscillations due to the shedding of blade-tip vorticity, prior to the far-outboard approach to a source-like decay of the velocity field. The unsteady influence of non-zero G is also discussed.

(b) *Non-symmetric pressure-wake interactions (mechanisms 2 and 3)*

This is aimed specifically at capturing mechanism 3. Two-dimensional flows past multiple thin blades positioned in near or exact sequence are studied by Smith & Timoshin (1996b). Non-symmetric blade arrangements yield the new global inner–outer interaction, as anticipated in § 3 a, in which the boundary layers, the wakes and the potential flow outside have to be determined together, to satisfy pressure-continuity conditions along each successive gap or wake. Thus the first blade in the sequence has a classical Blasius boundary layer, and, hence, the first wake is the same as that of an aligned flat plate, but its wake–centreline curve is unknown and so the second blade's boundary layer (and so on downstream) cannot be computed directly. Instead, the centreline curves can be guessed, to fix the viscous efflux V as in (3.2) in effect, which then fixes the upper and lower wake pressures, $\tilde{p}$, through the potential flow outside, and the differences between these two pressures can be used to revise the guesses for the centreline curves. The resulting iteration to solve (2.1) coupled with (3.2) captures the inner–outer interaction, which occurs at notably tiny angles of incidence for example. Smith & Timoshin (1996b) show results for various symmetric and non-symmetric arrangements, as well as observing quasi-periodic behaviour far downstream for many-bladed configurations. See figure 3 for a three-bladed non-symmetric configuration, where interesting distributions of pressure, shear, drag and lift (positive or negative) are found.

PHILOSOPHICAL TRANSACTIONS OF THE ROYAL SOCIETY A MATHEMATICAL, PHYSICAL & ENGINEERING SCIENCES

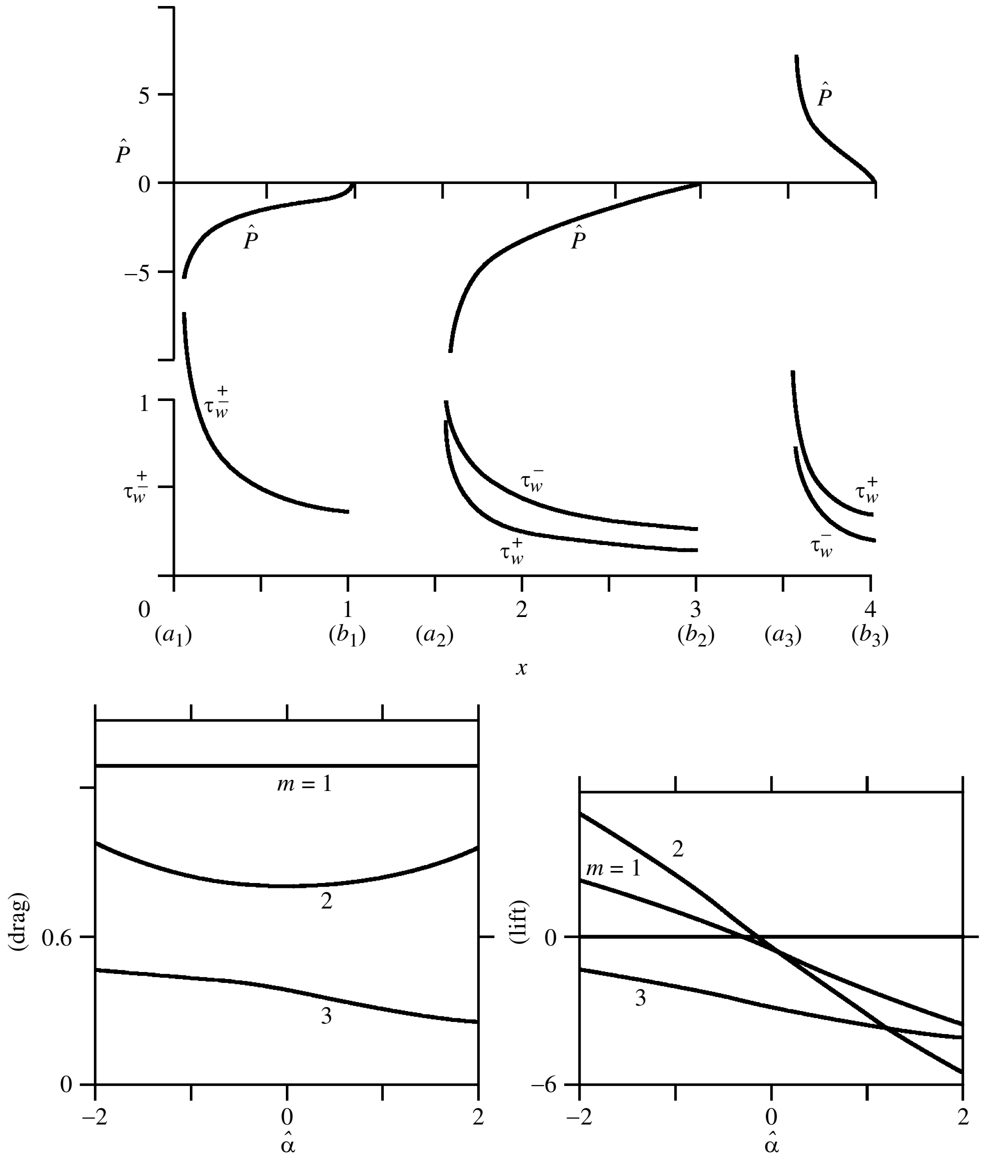

Figure 3. Plots of scaled wall shear $\tau_{\mathrm{W}}^{\pm}$, pressure $\hat{P}$ versus x, and of drag and lift, for a three-bladed non-symmetric arrangement (with non-symmetry parameter $\hat{\alpha}$) in planar pressure–wake interaction. The successive blades are $m = 1$, 2, 3.

(*c*) *Blades with pressure–displacement interaction (mechanisms 1 and 2)*

Pressure–displacement interaction for multiple successive blades and their wakes is incorporated in Bowles & Smith (2000*a*), for far-downstream motion, following estimates made by Smith & Timoshin (1996*b*). Again, the typical blade chord is $O(1)$, and three y-scales operate, of orders Re^{-m}, $m = 2/5$, $1/5$, 0, in triple-deck fashion. The task addressed in two dimensions is, therefore, to solve for the boundary layer (2.1) together with the boundary conditions (3.1 *d*) and (3.1 *e*) and interaction via (2.7 b), but here

$$p(x) = \frac{1}{\pi} \int_{-\infty}^{\infty} \frac{A'(\xi)\,\mathrm{d}\xi}{(x-\xi)}, \tag{3.3 a}$$

$$\text{streamwise periodicity in } x. \tag{3.3 b}$$

A periodic configuration of blades far downstream is a fairly representative arrangement. Mechanism 1 is present through (3.3 a), while mechanism 2 is implicit in (3.3 b). On the other hand, unlike most interactive flows involving mechanism 1 (e.g. see (a) in § 2), which are generally local in nature, the present interaction holds over the entire period and includes the whole blade and wake.

Figure 4a, b shows sample results with non-separated and separated flows present. The motions are y-symmetric, thus excluding mechanism 3. Further, the above paper finds that for relatively short blades, which give an extreme of practical concern, the flow with (3.3 a), (3.3 b) becomes multi-structured itself, inducing extra interactions between the short length-scale of the blade and the larger $O(1)$ scale of the wake and leading to a direct relation between the surface pressure p and the blade shape. This, in turn, resembling the relation derived in (2.5) and the following, provokes the Goldstein singularity on the leeward face of a sufficiently thick blade and then removal of the singularity and an ensuing breakaway separation from the blade, as in Smith & Daniels (1981).

(d) *With pressure–displacement interaction and non-symmetry (mechanisms 1–4)*

The subsequent work of Bowles & Smith (2000b) is as in § 3 c except that non-symmetry in y is allowed. Hence mechanism 3 enters, in addition to mechanisms 1 and 2. Moreover, another mechanism also emerges.

The same equations (2.1) and constraints, (3.1 d), (3.1 e) and (2.7 b), with (3.3 a), (3.3 b) apply here, above (+) and below (−) each blade and wake, supplemented by (3.2), in effect. Flow solutions are presented in figure 5a, b for a case of reduced length-scales, where A' is identically zero rather than as in (3.3 a). These solutions demonstrate the main features associated with *mechanism 4*, namely a pressure jump at each blade leading edge, such that

$$p(0-) \neq p^{\pm}(0+) \tag{3.4}$$

if the leading edge is at zero x, and a corresponding velocity jump and streamline discontinuity, when viewed from the current streamwise length-scales. The jumps or discontinuities are a product of the Kutta trailing-edge requirement and are smoothed out (removed) within a shorter length-scale near the leading edge, via a tiny Euler region of predominantly inviscid nonlinear adjustment. Other similar jumps are observed by Jones & Smith (2001), Smith & Jones (2000), in car-to-ground interactions and in internal branching flows, respectively, where the rapid adjustment necessary in the pressure is supported by the solid surfaces locally. In contrast, the support in the present context is provided by the uniform shears in the far-field, as in (2.7 b), essentially, and as explained by Bowles & Smith (2000b). We recall that these blades lie within the inner shear portion of a much larger, curved, input velocity profile, and this allows their flow characteristics to differ considerably from those of greater displaced blades.

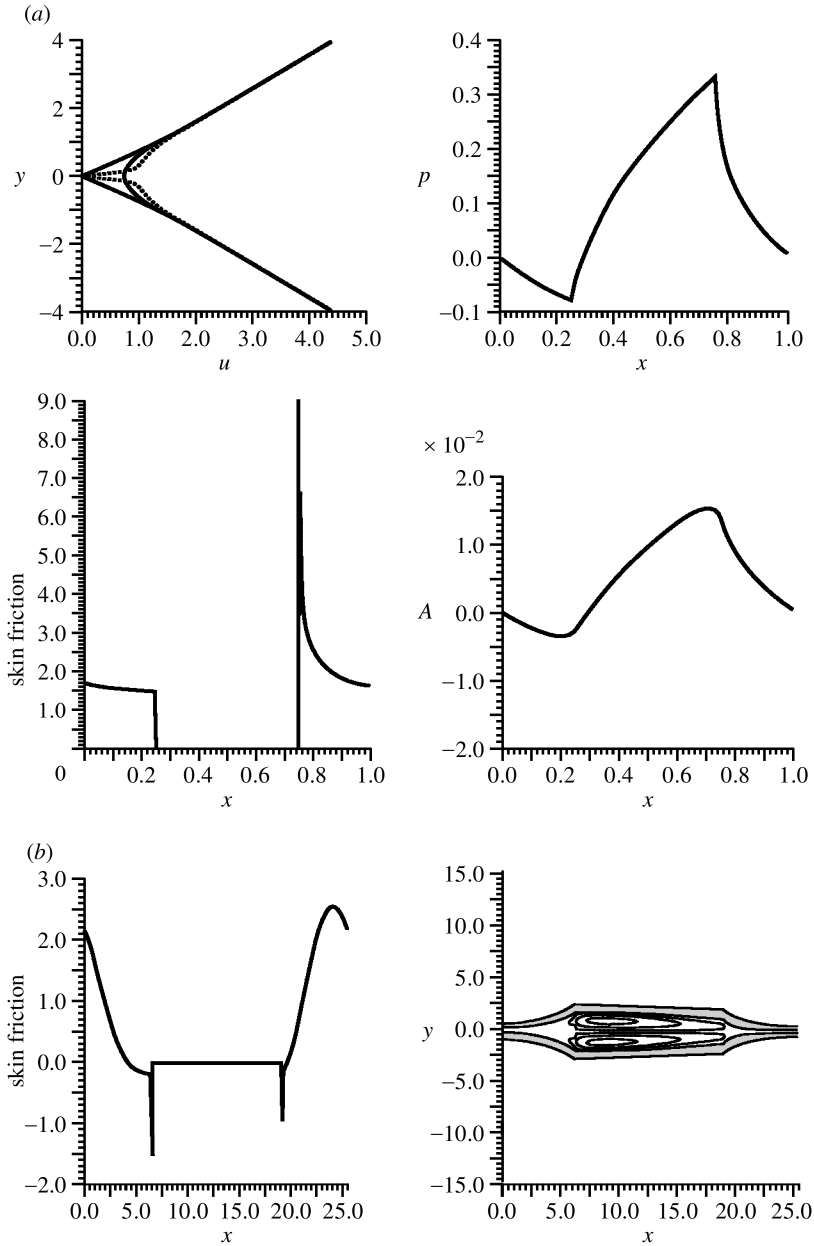

Figure 4. (*a*) Non-separated and (*b*) separated planar flow results for multiple blades with pressure–displacement interaction, streamwise periodicity and y-symmetry.

4. Flow past a three-dimensional roughness: mechanisms 5–7

(*a*) *A beginning, mechanism 5, and comparisons*

This section starts with two papers, Smith *et al*. (1977) and Smith (1976). The former considers the flow problem of an incident planar boundary layer encountering

PHILOSOPHICAL TRANSACTIONS OF THE ROYAL SOCIETY A MATHEMATICAL, PHYSICAL & ENGINEERING SCIENCES

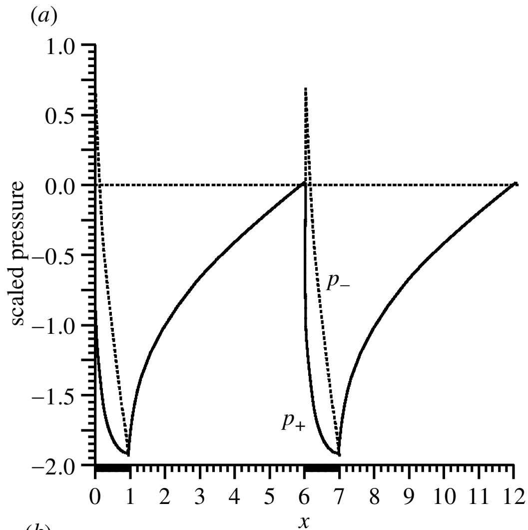

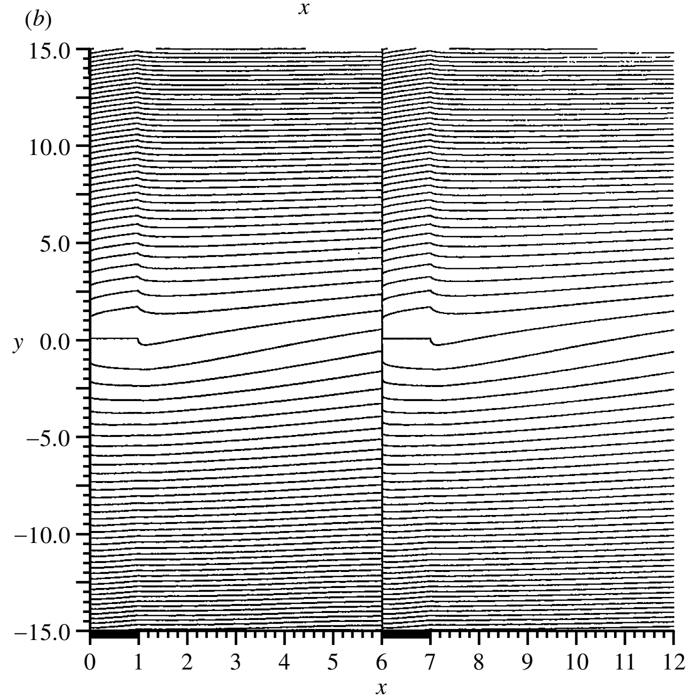

Figure 5. (*a*) Scaled pressure curves, (*b*) streamlines, indicating mechanism 4, associated with planar pressure–displacement interaction, streamwise periodicity but y-non-symmetry.

a three-dimensional obstacle mounted on the locally flat surface (figure 6), while the latter examines pipe flows distorted by non-symmetric indentation or other three-dimensional effect. A feature of wide interest is the generation of longitudinal vortices downstream, as well as the induced wall shear and pressure, and in particular we would like to know the origin of the strong horseshoe-type vortices so often observed in practice for a sufficiently pronounced roughness.

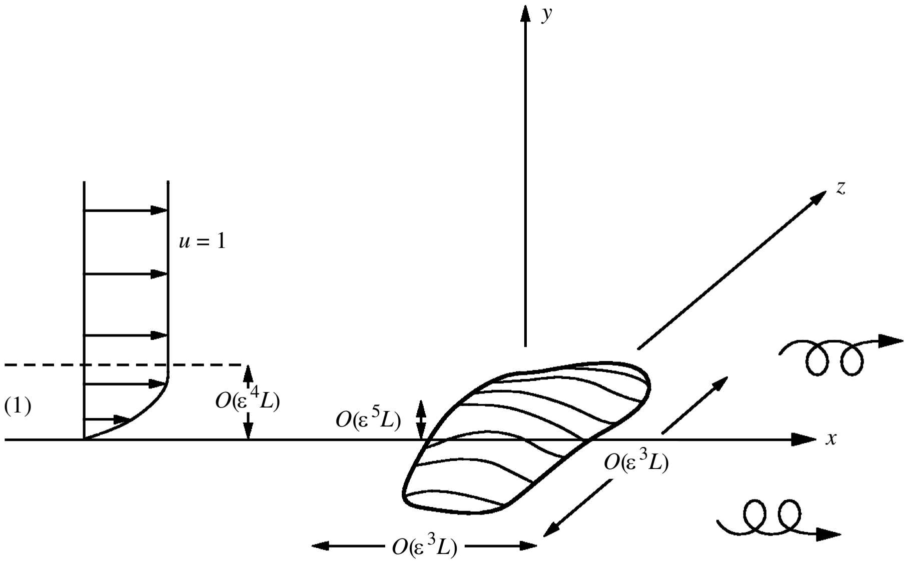

Figure 6. An oncoming planar boundary layer (1) encountering a three-dimensional roughness (shown shaded).

The equations of external motion for a roughness of triple-deck dimensions as given in Smith *et al.* (1977) and in figure 6 are the same as in (3.1 *a*)–(3.1 *c*) but with α zero, $(r, r\theta)$ replaced by scaled coordinates (X, Z), and $\partial/\partial t$ zero. The boundary conditions are mainly

$$\text{zero slip at } Y = hF(X, Z), \tag{4.1 a}$$

$$U \sim Y + A, \quad W \to 0 \quad \text{as } Y \to \infty, \tag{4.1 b}$$

$$P(X, Z) = -\frac{1}{2\pi} \int_{-\infty}^{\infty} \int_{-\infty}^{\infty} \frac{(\partial^2 A/\partial \xi^2)\, \mathrm{d}\xi \mathrm{d}\eta}{[(X-\xi)^2 + (Z-\eta)^2]^{1/2}}, \tag{4.1 c}$$

along with undisturbed shear flow in the far-field. Clearly, this involves a pressure–displacement interaction that, although three-dimensional, is from mechanism 1 at heart. Linearized results show the secondary vortex motion produced upstream of, over, around and downstream of the roughness, and in addition a ‘corridor’ of enhanced flow disturbance downstream (fig. 5 in Smith *et al.* (1977), for example), with spanwise length-scale comparable with that of the roughness itself, before the flow returns to its original planar state.

The trend of a corridor seems to be in agreement, qualitatively at least, with recent experiments of Buttsworth *et al.* (2000). Their skin friction measurements downstream of a three-dimensional roughness element in an incompressible laminar boundary layer show laminar effects persisting for distances of the order of many roughness widths, over a roughness Reynolds number range of 388–1360.

The second paper (Smith 1976) mentioned at the start of this section is on pipe flows, controlled by the same three-dimensional boundary-layer equations but with zero displacement,

$$A \equiv 0, \tag{4.2}$$

for so-called condensed flows of reduced streamwise length-scale; (4.2) then replaces (4.1 *c*). The paper actually also includes unsteady effects, which with pressure–displacement interaction yield Tollmien–Schlichting waves. The paper gives linearized solutions for the induced wall shears and pressure. Specifically, the linearized pressure formula in eqn (3.11) of Smith (1976) illustrates the solution dependence on the Laplacian $(P_{XX}+P_{ZZ})$, from adding together the X- and Z-derivatives of the X- and Z-momentum balances in turn. That addition serves to convert the three-dimensional problem into a two-dimensional parabolic one for the Laplacian, cf. Squire's theorem in linear stability theory. Integration for P then yields upstream influence, as in eqn (3.13a) in Smith (1976). This gives the specifically three-dimensional *mechanism 5*, an interaction and associated upstream influence which arise for all three-dimensional interactive boundary layers, whether spanwise periodic or not. In a sense, this mechanism is also present as a subcase of (4.1 *c*), but it is clearer for situation (4.2). Indeed, the background of this mechanism 5 is used to develop the 'skewed-shear method' of computing nonlinear solutions by Smith (1983), who obtained three-dimensional separations for both the full interaction (4.1 *c*) and the condensed case (4.2) (see his figs 1 and 3 and Smith (1986)). In fact, concerning nonlinear three-dimensional properties, the necessary numerical work was started earlier by Sykes (1980) and Smith (1980), adopting streamwise shooting in effect. This was followed by the skewed-shear method above, by pseudo-spectral techniques (Duck & Burggraf 1986), by Edwards *et al.*'s (1987) double-displacement methods, by Roget *et al.* (1998), and so on. Sykes's (1980) results, for three-dimensional flow over a surface irregularity in case (4.2), are both interesting and beautiful; for instance, the surface stress patterns and the perspective views of fluid particle trajectories in his figs 3 and 6, respectively.

(*b*) *Mechanism 6, and comparisons*

More recently, the more analytical approach of Smith & Walton (1998) and of F.T.S. with Professor S. N. Brown is taken with a view to understanding vortex production, especially in flow past a planar or three-dimensional roughness with steep edges. Concerning Smith & Walton (1998) first, much of their reasoning is quasi-planar but reveals three-dimensional flow structure. There are various parameter ranges as in their fig. 1, and the overall flows involve mechanisms 1 and 5 again but only in linear form. Of more interest is the case of strong or severe edges on the roughness, which can induce wall–layer separation well ahead of the edge or of a forward-facing step (as an example; see their fig. 4). The nonlinear mechanism involved here is *mechanism 6*. Discussing it, in three-dimensional motions, Smith & Walton (1998) observe the pressure feedback via an inviscid zone of square section, lying along the front face of the roughness and in which the flow is essentially a small perturbation of uniform shear motion provoked by the nonlinear pressure distribution generated on the roughness itself. In the nonlinear sublayer produced underneath the above zone, upstream of the roughness, we then have (2.1 *a*)–(2.1 *c*) again in a suitable cross-plane but together with the forcing constraint

$$u \sim y + \frac{\bar{h}^2}{\pi} \int_0^\infty \frac{\bar{f}(\xi)\bar{f}'(\xi)\,\mathrm{d}\xi}{(x-\xi)} \quad \text{as } y \to \infty, \tag{4.3}$$

as well as zero slip at zero y. Here $\bar{h}$, $\bar{f}$ denote the normalized height parameter and shape of the roughness, respectively. The pressure–feedback effect (4.3) on system (2.1 a)–(2.1 c) (etc.) leads to figs 3, 4, 10 and 11 in Smith & Walton (1998).

Mechanism 6 appears in earlier work by Smith (1978) and Dennis & Smith (1980) on axisymmetric and planar internal flows, respectively. The latter paper, on computations for symmetrically constricted channel flows, exhibits good quantitative agreement with the theory for Reynolds numbers above about 400 (Dennis & Smith, fig. 2, etc.), with respect to the upstream separation distance for instance. This distance at first decreases as *Re* increases for low *Re*, but then the trend reverses at higher *Re* in line with the theory. The mechanism is also evident in the subsequent computational results for internal flow of Durst & Loy (1985)—as seen, in their fig. 9, in the comparison of the upstream separation distance in front of an abrupt contraction—and Mei & Plotkin (1986); see their fig. 2 for separated streamlines in a channel and their fig. 3 for comparison of the upstream separation length, over a Reynolds-number range of 0–2000. The comparisons firmly support the theory.

Similarly, and more recently, interesting experimental investigations have been made by Giguère *et al.* (1997) on the 'Gurney flap' and its scaling concerning the lift-to-drag ratio of an airfoil. This flap is typically a tiny fence standing normal to the airfoil surface, near the trailing edge, as in their fig. 1. For a particular airfoil they note that Liebeck earlier found increased lift and reduced drag for high lift coefficients from the addition of a flap of height 1.25% chord, and the benefits of the device were maximized with heights between 1 and 2%. Results in broadly the same vein are given in their figs 1 and 2. Although they give the opinion that the physical mechanism associated with this device is still an open question, the present view is that it is the pressure–feedback mechanism 6 again.

(*c*) *Mechanism 7, and comparisons*

Returning to the Smith & Walton (1998) approach, we see another feature arising near a spanwise extremity or a 'wing-tip' of the three-dimensional roughness. The wing-tip area produces a nonlinear response governed by

$$\frac{\partial u}{\partial s}+\frac{\partial v}{\partial y}+\frac{\partial w}{\partial n}=0, \tag{4.4 a}$$

$$u\frac{\partial u}{\partial s}+v\frac{\partial u}{\partial y}+w\frac{\partial u}{\partial n}=0+\frac{\partial^2 u}{\partial y^2}, \tag{4.4 b}$$

$$u\frac{\partial w}{\partial s}+v\frac{\partial w}{\partial y}+w\frac{\partial w}{\partial n}-\kappa u^2=-\frac{\partial P}{\partial n}+\frac{\partial^2 w}{\partial y^2}, \tag{4.4 c}$$

in intrinsic coordinates, the pressure gradient being absent in (4.4 b) but present in (4.4 c), because the length-scale(s) along the roughness edge is (are) long compared with the scale n normal to the edge. Here κ is the wing-tip curvature $\mathrm{d}\bar{\beta}/\mathrm{d}s$ in planform, with $\bar{\beta}$ being the scaled angle between the x-axis, which is in the incident flow direction, and the tangent to the edge; the axis and tangent are nearly aligned in the wing-tip area. The boundary conditions require zero slip along $y=0$ and

$$(u,w)\sim(y+HF)(1,\bar{\beta}) \quad \text{as } y\to\infty, \tag{4.4 d}$$

along with appropriate matching at large negative s or positive n; H and F are the normalized height parameter and local roughness shape, respectively. This provides

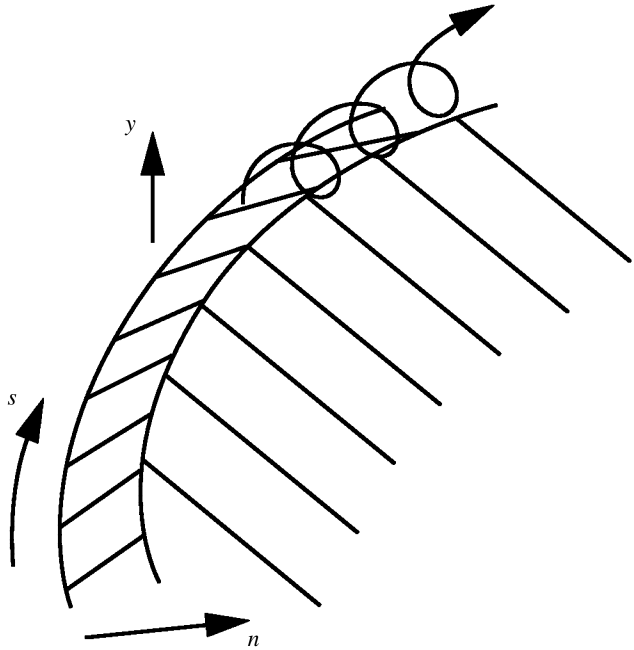

Figure 7. Three-dimensional flow pattern produced *on* the steep-edged roughness, inferred from fig. 9 in Smith & Walton (1998).

mechanism 7, a longitudinal effect that has a special form at nearly zero degrees alignment with the incident shear direction, as at a roughness wing-tip, where it incorporates the incident shear in a specifically three-dimensional interaction. The curvature terms seem almost incidental to the mechanism. The interaction remains parabolic in s and n prior to flow reversal setting in, as shown in fig. 9 of Smith & Walton (1998) for increasing values of H, which tend to hasten the reversal. The implication of that result is demonstrated in our figure 7, indicating longitudinal-like vortices being created on the roughness face as the distance s increases.

Qualitatively, the vortex results above from mechanism 7 are mildly encouraging in terms of understanding the generation of significant longitudinal vortices trailing from the roughness wing-tips. Quantitatively, there is more encouragement from mechanism 6 and its prediction for the ratio of the upstream separation distance over the roughness height,

$$0.142 Re_{\mathrm{W}}^{1/4} (\sin\beta)^{1/4}, \tag{4.5}$$

for severe edges, or forward-facing steps for example, in two or three dimensions. Here Re_{W} is the local Reynolds number based on roughness height and incident wall velocity slope, while β is the planform tangent angle (90° in the planar case). In a three-dimensional flow, the distance (4.5) is measured perpendicular to the forward face. Smith & Walton (1998) found that (4.5) is not in contradiction with the experiments of Klebanoff & Tidstrom (1972). Further, (4.5) is fairly close to the computational results of V. V. Bogolepov (1998, personal communication) on planar shear flow past a roughness for Re_{W} values of about 100 and beyond, as the upstream separation distance continues to increase, and there is similar quantitative agreement with computations by Bhattacharyya *et al.* (2000).

(*d*) *On horseshoe vortices*

The above calls to mind horseshoe vortices of a larger scale, such as those observed clearly and with much upstream influence in flow past a tall cylinder mounted in a boundary layer, as in figs 92 and 93 of Van Dyke (1982). The cylinder heights there exceed the incident boundary-layer thicknesses, whereas the present roughnesses are much shorter; nevertheless, the mechanism for the generation of larger-scale horseshoe vortices may be common, as follows.

Roughness heights increased beyond those appropriate for (4.4 *a*)–(4.4 *d*) are studied by F.T.S. with N. C. Ovenden, especially concerning the effects on the motion around the roughness, i.e. on the flat surface. A schematic is presented in figure 8*a*, this applying for H values much larger than $O(1)$ in effect. The flow structure has four regions (a)–(d). In the thin layer (a) on the roughness, the main property for present purposes is that the typical pressure increases as H^2, say $H^2\bar{P}(X,Z)$ in scaled terms. As an aside, examples of the flow solutions in (a) give three-dimensional marginal separations (Brown, Duck, Zametaev, Kluwick) and removal (Smith & Daniels) of the Goldstein singularity. The thin layer (b) downstream of (a) on the roughness is essentially passive, although it may generate vortices of the type described following (4.4 *d*). Sample numerical results for (a) are shown in figure 8*b*–*e*. Region (c), which is of square cross-section, couples the flow response on the roughness to that on the flat, by means of a small inviscid but three-dimensional perturbation of the incident uniform-shear motion. This leads to quasi-potential flow and, hence, to the relation

$$\partial_X^2(u_\mathrm{e}) = -\frac{1}{\pi}\int_{-\infty}^{0}\frac{\partial_\eta^3\bar{P}(X,\eta)\,\mathrm{d}\eta}{(Z-\eta)} \tag{4.6}$$

between the scaled slip velocity, u_e, induced on the flat and the pressure, $\bar{P}$, which is known from layer (a), on the roughness. The integral in (4.6) is over the range of layer (a) only, and the mixture of X and η derivatives is due to the elongated scale of region (c) compared with its cross-sectional length-scales. The nonlinear thin layer (d) induced on the flat then effectively has the governing equations (4.4 *a*)–(4.4 *c*) again, but with n being negative here and subject to the normalized outer condition

$$u \sim y + u_\mathrm{e} \quad \text{as } y \to \infty. \tag{4.7}$$

Thus, $u_\mathrm{e}(s,n)$ determined by (4.6) acts as a prescribed negative displacement, for the three-dimensional viscous response on the flat, upstream and around the roughness.

The description from (a)–(d) generates the necessary upstream influence near the wing-tip, unlike in (4.4 *a*)–(4.4 *d*), and it does so through the earlier pressure–feedback mechanism allied with the sensitive longitudinal effect from the near alignment with the shear at the wing-tip. Hence, this description incorporates the two mechanisms 6 and 7. It also applies more widely to flow skirting around a pressurized area. The suggested outcome is shown in figure 8*f*, indicating the generation of an increasingly strong vortex motion, possibly of breakaway-separation form in three dimensions, as X increases downstream. This suggestion follows from a double integration in X of (4.6), given boundedness constraints on the roughness-surface pressure $\bar{P}$, so that u_e then increases like X multiplied by a constant factor that is dependent upon a

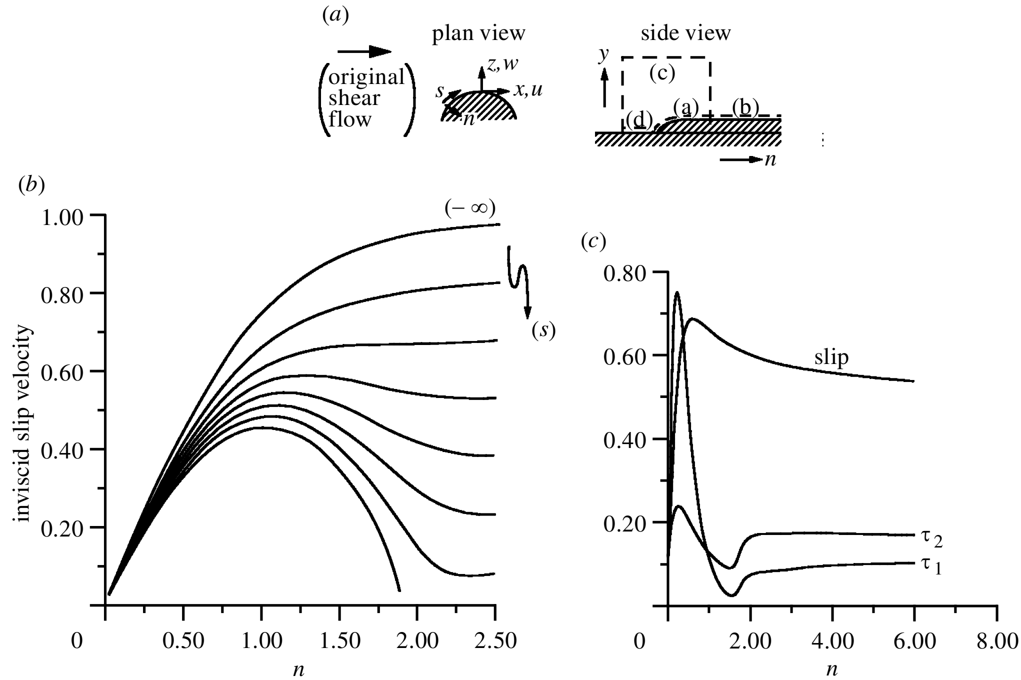

Figure 8. On the motion *around* the steep-edged roughness or more general pressurized area. (*a*) Plan view and side view of the flow structure near the wing-tip of the roughness. (*b*) Inviscid slip velocities, and (*c*)–(*e*) sample slip velocities and corresponding scaled wall shears (τ_1 and τ_2 in the n and s directions, respectively) for the three-dimensional motion on the roughness; the latter indicate marginal separation arising. (*f*) Anticipated flow pattern induced around the roughness, from (4.6), (4.7) and Smith *et al.* (2000), suggesting the creation of horseshoe vortices downstream.

local pressure integral. The full implications of such u_e behaviour are to be followed through in detail, but the overall effect, which increases linearly in strength beyond the roughness wing-tip, promises insight into the common formation of trailing horseshoe vortices.

5. Further comments

These will be kept brief. Much of the present paper has been on work in progress (§§ 3 and 4), while, in § 2, we note that other singularities associated with unsteady, moving-wall or three-dimensional classical boundary layers, for instance, lead to repercussions that are broadly analogous with mechanism 1. For multi-blade flows (§ 3), studies are continuing on the effects of non-symmetry, three dimensionality and unsteadiness, the last yielding some insight into near-wake transition (Smith *et al.* 2000) for velocity profiles such as that in figure 4*a*. For the surface-mounted roughness motions in § 4, transition is again of interest (see Savin *et al.* (1999), Allen *et al.* (1998), and references therein). Further, (4.6) can be enlarged to include the entire boundary-layer velocity profile; and the argument in § 4 *d* with mechanisms 6 and 7 may also apply for an entire roughness, over larger length-scales, and across an entire boundary layer.

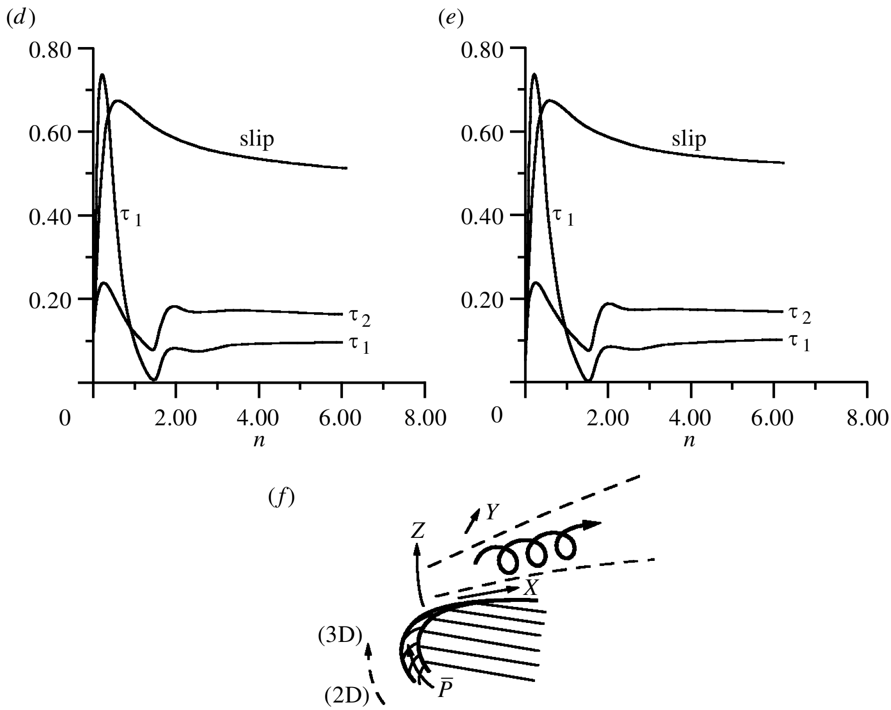

Figure 8. (*Cont.*) See opposite for description.

We conclude with the point that Goldstein's original work clearly caused a profitable re-examination of physical mechanisms in flows at high *Re*, and much more remains to be seen.

Thanks are due to the EPSRC and the MoD for support and to Alan Jones and many colleagues for their interest and comments. The referees' comments are gratefully acknowledged.

References

Allen, T., Brown, S. N. & Smith, F. T. 1998 An initial-value problem for fully three-dimensional inflectional boundary layer flows. *Theor. Comp. Fluid Dyn.* **12**, 131–148.

Bhattacharyya, S., Dennis, S. C. R. & Smith, F. T. 2000 Separating shear flow past a surface-mounted blunt obstacle. *J. Engng Math.* (In the press.)

Bowles, R. G. A. & Smith, F. T. 2000*a* Interactive flow past multiple blades and wakes. *Q. J. Mech. Appl. Math.* **53**, 207–251.

Bowles, R. G. A. & Smith, F. T. 2000*b* Lifting multi-blade flow with interaction. *J. Fluid Mech.* **415**, 203–226.

Brown, S. N. 1985 Marginal separation of a three-dimensional boundary layer on a line of symmetry. *J. Fluid Mech.* **158**, 95–111.

Brown, S. N. & Stewartson, K. 1969 Laminar separation. *A. Rev. Fluid Mech.* **1**, 45–72.

Buttsworth, D. R., Elston, S. J. & Jones, T. V. 2000 Skin friction measurements on reflective surfaces using nematic liquid crystals. *Exp. Fluids* **28**, 64–67.

Catherall, D. & Mangler, K. W. 1966 The integration of the two-dimensional laminar boundary-layer equations past the point of vanishing skin friction. *J. Fluid Mech.* **26**, 163–182.

Curle, N. 1962 *The laminar boundary layer equations.* Oxford University Press.

Dennis, S. C. R. & Smith, F. T. 1980 Steady flow through a channel with a symmetrical constriction in the form of a step. *Proc. R. Soc. Lond.* A **372**, 393–414.

Duck, P. W. & Burggraf, O. R. 1986 Spectral solutions for three-dimensional triple-deck flow over surface topography. *J. Fluid Mech.* **162**, 1–22.

Durst, F. & Loy, T. 1985 Investigations of laminar flow in a pipe with sudden contractions of cross sectional area. *Comp. Fluids* **13**, 15–36.

Edwards, D. E., Carter, J. E. & Smith, F. T. 1987 Analysis of three-dimensional separated flow with the boundary-layer equations. *AIAA J.* **25**, 380–387.

Elliott, J. W. & Smith, F. T. 1985 On the abrupt turbulent reattachment downstream of leading-edge laminar separation. *Proc. R. Soc. Lond.* A **401**, 1–27.

Giguère, P., Dumas, G. & Lemay, J. 1997 Gurney flap scaling for optimum lift-to-drag ratio. *AIAA J.* **35**, 1888–1890.

Goldstein, S. 1948 On laminar boundary-layer flow near a position of separation. *Q. J. Mech. Appl. Math.* **1**, 43–69.

Hartree, D. R. 1937 On an equation occurring in Falkner and Skan's approximate treatment of the equations of the boundary layer. *Proc. Camb. Phil. Soc.* **33**, 223–239.

Howarth, L. 1938 On the solution of the laminar boundary layer equations. *Proc. R. Soc. Lond.* A **164**, 547–564.

Jones, M. A. & Smith, F. T. 2001 Fluid motion for car undertrays in ground effect. *Phil. Trans. R. Soc. Lond.* A **359**. (In the press.)

Klebanoff, P. S. & Tidstrom, K. D. 1972 Mechanism by which a two-dimensional roughness element induces boundary layer transition. *Phys. Fluids* **15**, 1173–1188.

Kluwick, A.F. 1998 On marginally separated flows in dilute and dense gases. In *Proc. IUTAM Symposium, Manchester, 6–9 July 1998.*

Lighthill, M. J. 1953 On boundary layers and upstream influence. II. Supersonic flows without separation. *Proc. R. Soc. Lond.* A **217**, 478–507.

Mei, R. W. & Plotkin, A. 1986 Navier–Stokes solutions for laminar incompressible flows in forward-facing step geometries. *AIAA J.* **24**, 1106–1111.

Messiter, A. F. 1970 Boundary layer flow near the trailing edge of a flat plate. *SIAM J. Appl. Math.* **18**, 241–257.

Neiland, V. Ya. 1969 Towards a theory of separation of the laminar boundary layer in a supersonic stream. *IZV Akad. Nauk. SSSR, Mekh. Zhidk. Gaza* **4**, 53–57.

Oswatitsch, K. & Wieghardt, K. 1941 German wartime report. Reprinted as Tech. Memo. Nat. Adv. Comm. Aero., Wash., no. 1189 (1948).

Roget, C., Brazier, J. Ph., Cousteix, J. & Mauss, J. 1998 A contribution to physical analysis of separated flows past three-dimensional humps. *Eur. J. Mech.* **17**, 173–211.

Ruban, A. I. 1981 Singularity solution of boundary-layer equations which can be extended continuously through the point of zero skin friction. *Izv. Akad. Nauk. SSSR, Mech. Zhidk. Gaza* **6**, 42–52.

Ruban, A. I. 1982 Asymptotic theory of short separation bubbles on the leading edge of a thin airfoil. *Izv. Akad. Nauk. SSSR, Mech. Zhidk. Gaza* **1**, 42–51.

Savin, D. J., Smith, F. T. & Allen, T. 1999 Transition of free disturbances in inflectional flow over an isolated roughness. *Proc. R. Soc. Lond.* A **455**, 491–541.

Smith, F. T. 1976 Pipeflows distorted by non-symmetric indentation or branching. *Mathematika* **23**, 62–83.

Smith, F. T. 1978 Flow through symmetrically constricted tubes. *J. Inst. Math. Applic.* **21**, 145–156.

Smith, F. T. 1980 A three-dimensional boundary-layer separation. *J. Fluid Mech.* **99**, 185–224.

Smith, F. T. 1982 Concerning dynamic stall. *Aeronaut. Q.* **November**, 331–352.

Smith, F. T. 1983 Properties, and a finite-difference approach, for interactive three-dimensional boundary layers. Utd. Techn. Res. Cent. report No. 83-46.

Smith, F. T. 1986 Steady and unsteady boundary-layer separation. *A. Rev. Fluid Mech.* **18**, 197–220.

Smith, F. T. & Daniels, P. G. 1981 Removal of Goldstein's singularity at separation, in flow past obstacles in wall layers. *J. Fluid Mech.* **110**, 1–37.

Smith, F. T. & Jones, M. A. 2000 One-to-few and one-to-many branching tube flows. *J. Fluid Mech.* **423**, 1–31.

Smith, F. T. & Timoshin, S. N. 1996*a* Blade–wake interactions and rotary boundary layers. *Proc. R. Soc. Lond.* A **452**, 1301–1329.

Smith, F. T. & Timoshin, S. N. 1996*b* Planar flows past thin multi-blade configurations. *J. Fluid Mech.* **324**, 355–377.

Smith, F. T. & Walton, A. G. 1998 Flow past a two- or three-dimensional steep-edged roughness. *Proc. R. Soc. Lond.* A **454**, 31–69.

Smith, F. T., Sykes, R. I. & Brighton, P. W. M. 1977 A two-dimensional boundary layer encountering a three-dimensional hump. *J. Fluid Mech.* **83**, 163–176.

Smith, F. T., Bowles, R. G. A. & Li, L. 2000 Nonlinear effects in absolute and convective instabilities of a near-wake. *Eur. J. Mech.* B **19**, 173–211.

Stewartson, K. 1958 On Goldstein's theory of laminar separation. *Q. J. Mech. Appl. Math.* **11**, 339–410.

Stewartson, K. 1970 Is the singularity at separation removable? *J. Fluid Mech.* **44**, 347–364.

Stewartson, K. & Williams, P. G. 1969 Self-induced separation. *Proc. R. Soc. Lond.* A **312**, 181–206.

Stewartson, K., Smith, F. T. & Kaups, K. 1982 Marginal separation. *Stud. Appl. Math.* **67**, 45–61.

Sykes, R. I. 1980 On three-dimensional boundary layer flow over surface irregularities. *Proc. R. Soc. Lond.* A **373**, 311–329.

Timoshin, S. N. 1997 Leading edge receptivity in three-dimensional classical boundary layers. *Eur. J. Mech.* B **16**, 409–437.

Van Dyke, M. 1982 *An album of fluid motion.* Stanford, CA: Parabolic Press.

Zametaev, V. B. & Kravtsova, M. A. 1998 Influence of a thin inviscid longitudinal vortex on two-dimensional preseparated boundary layer. In *Proc. Euromech Colloquium, Manchester, 6–9 July 1998.*